World Academy of Science, Engineering and Technology
International Journal of Aerospace and Mechanical Engineering
Vol:8, No:6, 2014

Influence Analysis of Pelamis Wave Energy Converter Structure Parameters

Liu Shengnan, Sun Liping, Zhu Jianxun

***Abstract*—**Based on three dimensional potential flow theory and hinged rigid body motion equations, structure RAOs of Pelamis wave energy converter is analyzed. Analysis of numerical simulation is carried out on Pelamis in the irregular wave conditions, and the motion response of structures and total generated power is obtained. The paper analyzes influencing factors on the average power including diameter of floating body, section form of floating body, draft, hinged stiffness and damping. The optimum parameters are achieved in Zhejiang Province. Compared with the results of the pelamis experiment made by Glasgow University, the method applied in this paper is feasible.

***Keywords*—**Pelamis, Hinge, Floating multibody, Wave energy.

I. Introduction

THE Pelamis is a wave energy converter (WEC) developed and manufactured by Pelamis Wave Power, a Scottish based company. The Pelamis is a semi-submerged wave energy converter with a simple geometry configuration based on individual cylindrical segments linked linearly by hinged joints. As waves pass down the length of the machine, the induced motions of the separate segments relative to one another are resisted by hydraulic rams. Main tube cylinders are separated at each joint by shorter Power Conversion Module's (PCM's), and it transports power to the coast and power grid through the flexible connector and the high voltage cable connection under the sea.

The Pelamis WEC concept embodies a number of sophisticated hydrodynamic and engineering principles that give it a decisive competitive advantage over all other WEC concepts. Different from other kinds of WECs, Pelamis effectively balances the conflicting requirements of survivability in the harsh marine environment, and power capture efficacy in small seas. And the long thin form of Pelamis gives it the highest water-plane area to volume ratio of any WEC system under development. Water-plane area is the primary driver for power capture in small seas and volume is a basic indicator of weight and cost. Then Pelamis is the only WEC system that reacts against its own body, rather than against a separate external reaction frame such as the seabed or a large internal or external weight. This has the double advantage of readily allowing loads to be limited in extreme conditions, and the removal of significant costs associated with the provision of an external source of reaction. On the other hand, Pelamis introduces the concept of 'tuneable resonant response' to its performance-cross-coupled resonant response only when desired, the default or natural condition is a benign, non-resonant response capable of dealing with extreme conditions.

Babarit [1] mentioned that for devices that have been publicly announced, the available information is usually limited to sketches, pictures and animations, and in some cases, also dimensions and system layout. Only a few quantitative figures on the estimated or measured energy conversion are presently known. Danish Wave Energy Research program [2] resulted in estimates of energy absorption and cost estimates for 15 different WECs which were obtained through tank test experiments. It was shown that for all the considered devices, the capture width ratio1 varied between 4 and 30%. Estimates for the cost of energy for prototypes indicate to be at best about 1 V/kWh. Energy delivery and costs of 8 devices were assessed for potential deployment in a pilot plant in the US regarding energy production and costs [3]. The methodology was based on information given by the developers. The study concluded that only the Pelamis was acceptable for selection at that time.

Pelamis is composed of hinged semi-submersible cylinders, the research on semi-submersible slender floating body and hinged floating body provided important theoretical support for the development of Pelamis. Manases [4] introduced common WECs floating body and made numerical simulation in the report, the results show that the resonance cycle and roll motion amplitude of the floating body depends on metacentric height, and additional inertia moment and the structure inertia moment. Then simulating floating body in the regular wave by wamit, and predicting the motion response of the real sea condition. Nicolai F. etc.[5] used nonlinear numerical calculation for the horizontal slender cylindrical floating bodies based on the incompressible Navier-Stokes equations, taking into account the 6 degrees freedom coupled motion of floating body and complicated boundary conditions, the natural period of floating body, added mass, damping, and compares the results with the potential flow theory. Newman [6] used boundary integral method, calculated motion response of two hinged floating box, considering these two hinged box as a system with seven degrees freedom. In this way can it greatly reduce the amount of calculation and storage capacity of computer. GouYing, Teng Bin, etc. [7] used boundary integral equation method to study the interaction problem of wave and two three dimensional floating body. Considering the floating body hydrodynamic interference in the calculation, floating body motion response was achieved through the motion equations and continuity conditions of floating body. Then the results

Liu Shengnan is with the Ship Building Engineering Department, Harbin Engineering University, Harbin, CO 150001China (phone: 8615124517550; fax: 86-0451-82569359; e-mail: xiaonan003@163.com).

Sun Liping and Zhu Jianxun are with the Ship Building Engineering Department, Harbin Engineering University, Harbin, CO 150001China (e-mail: sunliping@hrbeu.edu.cn, hualishu2@163.com)

were compared with Newman.

II. Methods

Assuming fluid is irrotational, viscous, incompressible ideal fluid, and satisfy potential flow theory, the incident potential is known, wave height is small enough, wave satisfy the linear wave theory. Considering the system is composed of n hinged floating bodies, the overall coordinate and local coordinates are as shown in Fig. 1.

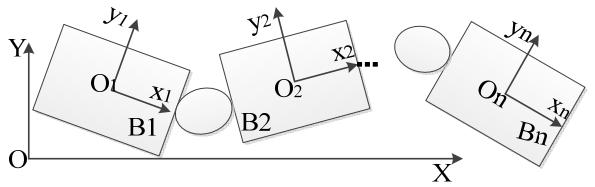

Fig. 1 Coordinate systems

A. Motion Responses

The motion responses amplitude should be determined by rigid body motion equation [8]:

$$-\omega^2 M\xi - i\omega B\xi + K\xi = f + f_m + f_e \tag{1}$$

where, M is the mass matrix of the object, B is the damping matrix of the object, K is the stiffness matrix of mooring system, ξ is displacement vector, f is the fluid forces, f_m is gravity part of the object, f_e is the static parts of the external mooring system. Considering the objects stay in a stationary state under the action of hydrostatic pressure, gravity and external static mooring force, (1) can be rewritten as:

$$\left(-\omega^2(M+a) - i\omega(B+b) + (K+C)\right)\xi = f_{ex} + f_e \tag{2}$$

where, f_{ex} is the exciting force, C is the restoring force matrix, a is additional mass matrix, b is the radiation damping matrix. Neglected the damping matrix of system and the external constraints, two adjacent objects of the system B_i, B_{i+1} respectively satisfy the motion equation as follows:

$$\begin{aligned}&\left(-\omega^2(M_{Bi} + a_{BiBi}) - i\omega b_{BiBi} + C_{Bi}\right)\xi_{Bi} + \\ &(-\omega^2 a_{BiBi+1} - i\omega b_{BiBi+1})\xi_{Bi+1} = f_{exBi} + F_{Li\sim i+1} - F_{Li-1\sim i}\end{aligned} \tag{3}$$

$$\begin{aligned}&\left(-\omega^2(M_{Bi+1} + a_{Bi+1Bi+1}) - i\omega b_{Bi+1Bi+1} + C_{Bi+1}\right)\xi_{Bi+1} + \\ &(-\omega^2 a_{Bi+1Bi} - i\omega b_{Bi+1Bi})\xi_{Bi} = f_{exBi+1} - F_{Li\sim i+1} + F_{Li+1\sim i+2}\end{aligned} \tag{4}$$

where, f_{exBi}, f_{exBi+1} is the wave force on object B_i, B_{i+1}, M_{Bi}, M_{Bi+1} is the mass matrix of object B_i, B_{i+1}, C_{Bi}, C_{Bi+1} is restoring force matrix of object B_i, B_{i+1} respectively, a_{ij}, b_{ij} is the added mass and radiation damping of object j as a result of the motion of object i, $F_{Li\sim j}$ is connection force of object i and object j. For rigid hinged connection, if it can't limit one direction movement of the object, then the corresponding binding force is zero. Two hinged objects only turn around Y axis freely, then the hinged binding component is expressed as:

$$F_{Li\sim j} = (F_{L1}, F_{L2}, F_{L3}, F_{L4}, 0, F_{L6})^T \tag{5}$$

Considering the displacements continuity conditions at the edges of hinge joint, displacement and angle equation of connection point can be achieved by two local coordinate systems.

$$\begin{aligned}&x_i + \varepsilon\left[\xi_i + a_i \times (x_i - x_{Oi})\right] \\ &= x_{i+1} + \varepsilon\left[\xi_{i+1} + a_{i+1} \times (x_{i+1} - x_{O(i+1)})\right], \\ &\alpha_{ix} = \alpha_{(i+1)x}, \alpha_{iz} = \alpha_{(i+1)z}\end{aligned} \tag{6}$$

where, x_i, x_{i+1} is coordinate of join point in two local coordinates, x_{Oi}, $x_{O(i+1)}$ is local coordinate of two objects' rotation center, ξ_i , ξ_{i+1} is translational displacement, α_i, α_{i+1} is angle displacement, α_{ix}, $\alpha_{(i+1)x}$,α_{iz},$\alpha_{(i+1)z}$ is angular displacement of B_i, B_{i+1} in X and Z directions. After the equations of two arbitrary adjacent objects of the system are constructed, motion response of the objects and constraint reaction force can be achieved.

B. Generated Power

When relative angle between two buoy is much small comparing to the dimension of buoy. Relative angle can be written as $\theta = \bar{X}/r, \dot{\theta} = \bar{V}/r$. And hinged moment can be written as follows.

$$M = K_\theta\theta + C_\theta\dot{\theta} \doteq C_\theta\dot{\theta} \tag{7}$$

where, r is the distance between pneumatic cylinder and axis of buoy, $\bar{X}$、$\bar{V}$ is average linear displacement and linear velocity in pneumatic cylinder position, K_θ, C_θ is rotation stiffness and damping.

Average power can be expressed as follows:

$$\bar{P} = M \cdot \dot{\theta} = \left(C_\theta\dot{\theta}\right)\dot{\theta} = C_\theta \bar{V}^2 / r^2 \tag{8}$$

Assumes that the expression of relative angular velocity is $\dot{\theta}(t) = A_0 \sin(\omega t)$, then average power can be written as:

$$\bar{P} = \frac{1}{T}\int_0^T C \cdot A_0^{\,2} \sin(\omega t)\, dt = \frac{1}{2} C \cdot A_0^{\,2} \tag{9}$$

A_0 is angular velocity amplitude. Considering different sea state probability, total average power can be expressed as the sum of power in single sea condition times probability factor.

$$P_T = \sum_{i=1}^{N} \eta_i \bar{P}_i \tag{10}$$

N is total number of sea conditions, η is probability factor.

III. Basic Parameters of Device

A. Structural Parameters of Floating Body

Plane xoy in all states is parallel to water plane and goes through the center axis of the cylinder, z axis is vertical. Global coordinate, hinged coordinate and cross section sketch map are shown in Figs. 2 and 3, the principal dimensions and parameters are shown in Table I.

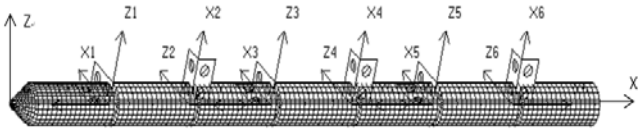

Fig. 2 Coordinate System

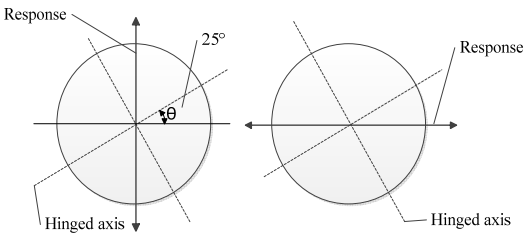

Fig. 3 Hinged axis in both ends

TABLE I
Sizes and Parameters of the Benchmark Device

Total length of device[m]	66.5
Number of floating bodies	7
Spacing between floating bodies[m]	0.6
Diameter of floating body[m]	3.5
Diameter of front end[m]	0.35
Total weight of device[t]	377.9
Hinged stiffness[N*m/rad]	4.49E6
Hinged damping[N*m/rad/s]	2.25E7
Draft[m]	2.1
Height of gravity center[m]	1.75
Water depth[m]	37

B. Parameters of Mooring System

In the numerical simulation, the mooring system of Pelamis is in the form of linear mooring with stiffness 2E6 as shown in Fig. 4. No.1, No.2 mooring line are connected to the Structure 1, No.3, No.4 mooring line are connected to the Structure 5. The angle of mooring line and structure is 45°.

C. Sea Conditions

Offshore wave energy distribution of Chinese provinces is shown as Fig. 5 [9].

Zhejiang Province has the most wave energy in mainland, especially the middle part of Zhejiang. Then the middle part of Zhejiang is chosen as the operate site of device. According to sea conditions probability distribution in its operating sea area, ten sea conditions with the highest probability are chosen to calculate [10]. Wave spectrum is JONSWAP spectrum, wave direction is along the x axis.

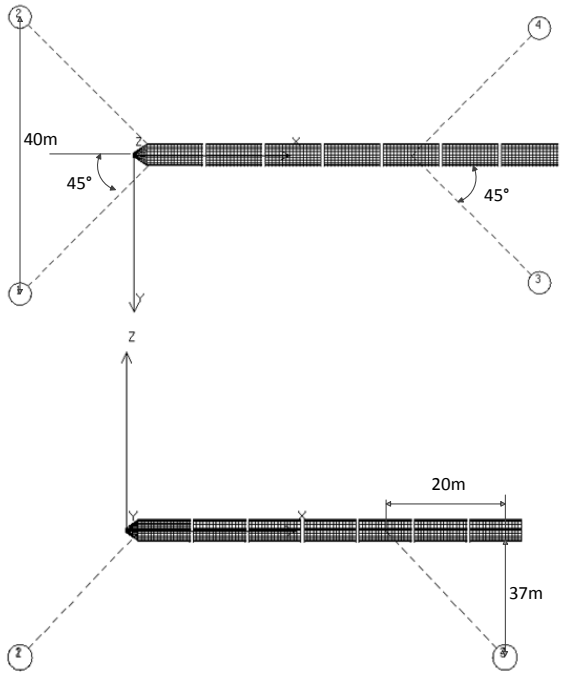

Fig. 4 Mooring System

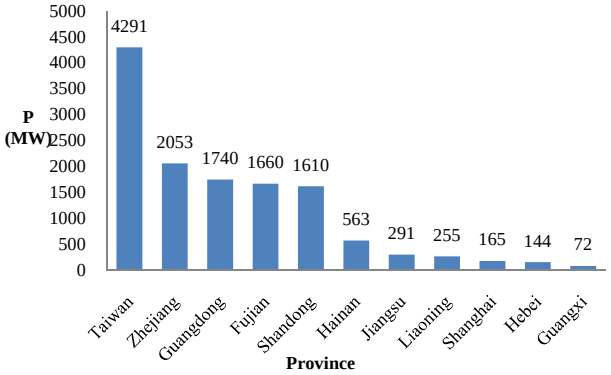

Fig. 5 Wave energy distribution

TABLE II
Significant Wave Height-Peak Spectral Period Probability Distribution (%)

T(s) / H(m)	5	5.5	6	6.5	7	7.5
4.5						0.14
4					0.14	0.07
3.5					0.07	0.07
3				0.61	0.75	0.14
2.5				2.66	0.41	
2			9.08	3.28	0.34	
1.5		8.67	20.36	2.94	0.61	
1	1.71	28.89	14.41	0.68		
0.5	2.05	1.64	0.07			

IV. Numerical Simulation

A. Analysis of Floating Body Motion

Sway and heave RAO of floating body play a major role in device's generated power. The Sway and heave RAO of benchmark device's floating bodies are shown in Figs. 6 and 7.

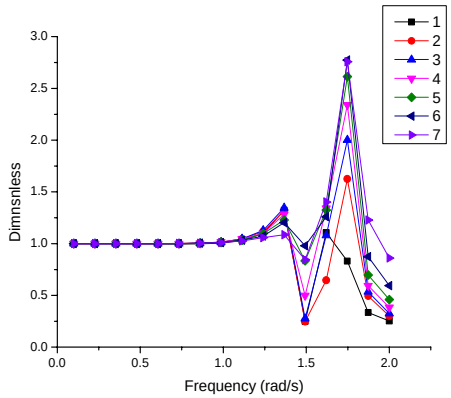

Fig. 6 Heave RAO in 0°wave direction

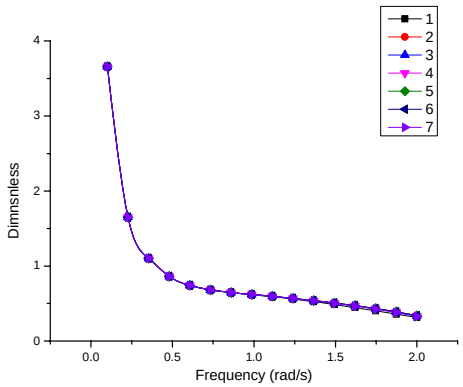

Fig. 7 Sway RAO in 45°wave direction

In the condition of head sea, vertical motion is predominant, and heave response can reach crest value near frequency 1.75 rad/s. In the condition of oblique sea, the floating bodies' sway RAO differ little, decreases with increasing wave frequency. The device is simulated in free floating state without the influence of the mooring system [11], [12].

B. Influence Analysis of Parameters

AQWA-FER is used to make numerical calculation on the device. Relative velocity response spectrum can be achieved between two adjacent floating bodies in cylinder position, as shown in Fig 8.

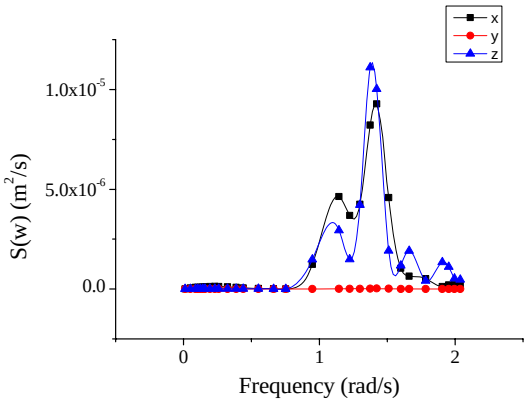

Fig. 8 Spectra of relative velocity

On the basis of related theory of spectrum analysis, the average speed can be written as $\bar{V} = 1.25\sqrt{A}$ [13], A is the area that spectra density curve contains. And the average generated power can be achieved through (9) and (10).

Diameter of Floating Body

To study the effect of diameter on power absorption, parameters expect diameter of benchmark model remain unchanged, select respectively the diameter of 3.5m, 4.0m, 4.5m, 5.0m to complete model calculation. The curve that average power varies with the diameter is shown in Fig. 9 and Table III lists the power value.

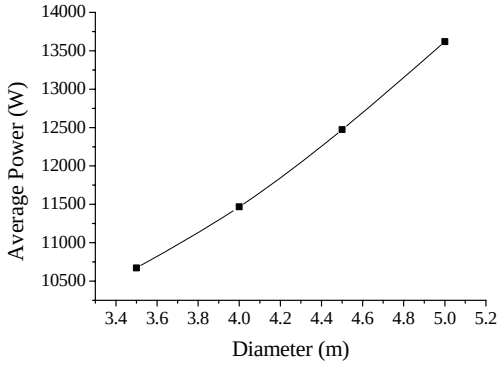

Fig. 9 Average power—Diameter

TABLE III
AVERAGE POWER—DIAMETER

Diameter(m)	3.5	4	4.5	5
Power(W)	1.07E+04	1.15E+04	1.25E+04	1.36E+04

It can be seen that the power increases with the increase of diameter. When diameter increases, the inertia and wave capture width of the device increases, then the absorption of energy increases. In actual production, considering the equipment layout and cost restrictions, there will be a certain selection scope of diameter. Weighing the potential benefits by increasing diameter against the increase of cost, we can get the diameter corresponding to greatest benefit.

Section Form of Floating Body

Considering the influence of section form on power absorption, parameters keeps coherent with benchmark model, cross section is set to ellipse. Complete model calculation when the ratio of major and minor axes is 1.5, 2.0, 2.5, 3.0 (Keep elliptic section area same with benchmark model, parameters are shown in Table IV). Table V lists the power in different ratios of major and minor axes. The curve of average power varies is shown in Fig. 10.

TABLE IV
ELLIPTIC SECTION PARAMETERS

Ratio of major and minor axes	Horizontal major axes [m]	Vertical minor axes [m]
1.5	4.29	2.86
2	4.95	2.47
2.5	5.53	2.21
3	6.06	2.02

TABLE V
AVERAGE POWER—RATIO OF MAJOR AND MINOR AXES

a/b	1	1.5	2	2.5	3
Power(W)	1.07E+04	1.28E+04	1.47E+04	1.67E+04	1.86E+04

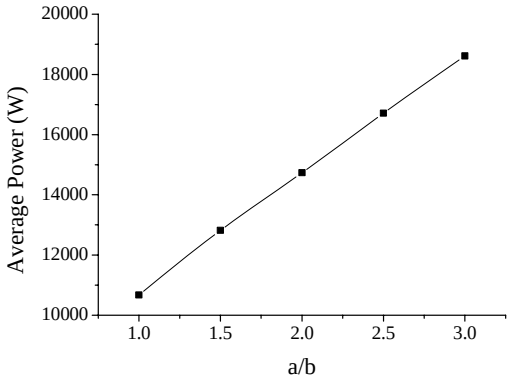

Fig. 10 Average power—Ratio of major and minor axes

The average power of the device increases with the increase of ratio of major and minor axes. It means that the device with elliptic section has higher average power than circular section. The wave capture width increases with the increase of ratio of major and minor axes, and the more flat the device is, the more excellent motion performance in sway is. These all lead to the increase of the power. Main restriction on cross section form is the equipment arrangement; it limits the minimum diameter of the device generally. After determine the minor axe length, major axe length can be determined according to the same area with circular cross section.

Draft

To study the effect of draft on power absorption, select respectively the draft of 0.5D, 0.6D, 0.7D and 0.8D. Table VI lists the power in different drafts. The curve that average power varies with draft is shown in Fig. 11.

TABLE VI
AVERAGE POWER—DRAFT

Draft	0.5D	0.6D	0.7D	0.8D
Power(W)	1.08E+04	1.07E+04	1.14E+04	1.15E+04

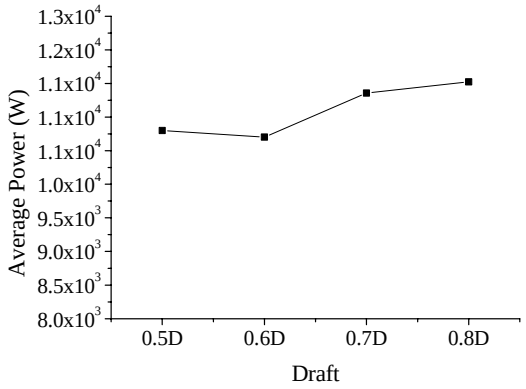

Fig. 11 Average power—Draft

In general, the change of the draft does not have much effect on average power. Average power reaches maximum at the draft 0.8D and its value is close to power of draft 0.7D. The water plane stiffness decreases with the draft increasing, and the motion will be more severe. The water plane stiffness changes little between 0.5D and 0.6D draft, but decrease obviously from 0.6D to 0.8D. Considering unsinkability and stability and little power increment of larger draft, the draft 0.5D to 0.6D is suggested.

Hinged Stiffness and Damping

If the device is too hard, the relative motion will be not enough to absorb wave energy effectively, if the device is too soft, the conversion of hydraulic energy is limited. So the proper hinged stiffness and damping is of great concern. Choose benchmark model and sea condition with the highest probability (significant wave height is 1.0 m, peak spectral period is 5.5s). At first, keep damping C=1E5, 1E6, 1E7 and 1E8 respectively, stiffness K is changed from 1E2 to 1E8, The trend that average power varies with K is shown in Fig. 12 and Table VII.

TABLE VII
AVERAGE POWER—HINGED STIFFNESS (W)

C / K	1.00E+05	1.00E+06	1.00E+07	1.00E+08
1.00E+02	5.78E+02	2.90E+03	2.08E+03	1.02E+03
1.00E+03	5.76E+02	2.90E+03	2.08E+03	1.02E+03
1.00E+04	5.72E+02	2.88E+03	2.08E+03	1.02E+03
1.00E+05	5.39E+02	2.80E+03	2.08E+03	1.02E+03
1.00E+06	6.62E+02	2.18E+03	2.16E+03	1.02E+03
1.00E+07	3.85E+01	3.27E+02	1.29E+03	1.02E+03
1.00E+08	1.18E+00	1.18E+01	1.14E+02	7.12E+02

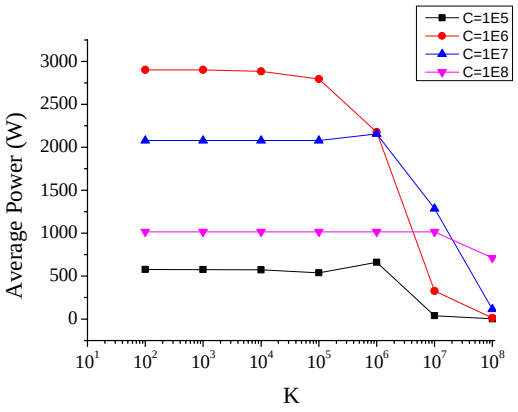

Fig. 12 Average power—Hinged stiffness

It can be predicted that a maximum average power appears as magnitude of C is near 1E6. And when C is 1E5 and 1E7, average power reaches to the maximum when K is 1E6. When K<1E5, the change of k has little effect on average power. Sampling between K=1E5 and 1E7 peak value can be achieved when K=9E5. Then keep K=1E4, 1E5 and 9E5 respectively, damping C is changed from 1E2 to 1E8. Table VIII lists the power in different hinged damping. And the trend that average power varies with damping C is shown in Fig. 13.

TABLE VIII
AVERAGE POWER—HINGED DAMPING (W)

C \ K	9.00E+05	1.00E+05	1.00E+04
1.00E+04	1.57E+02	5.84E+01	6.19E+01
1.00E+05	6.00E+02	5.39E+02	5.72E+02
3.00E+05	1.17E+03	1.39E+03	1.46E+03
5.00E+05	1.58E+03	1.99E+03	2.08E+03
7.00E+05	1.89E+03	2.40E+03	2.50E+03
1.00E+06	2.22E+03	2.80E+03	2.88E+03
1.50E+06	2.59E+03	3.08E+03	3.11E+03
3.00E+06	2.73E+03	2.98E+03	3.02E+03
3.50E+06	2.73E+03	2.94E+03	2.97E+03
4.00E+06	2.61E+03	2.86E+03	2.96E+03
6.00E+06	2.46E+03	2.54E+03	2.54E+03
1.00E+07	2.16E+03	2.08E+03	2.08E+03
1.00E+08	1.02E+03	1.02E+03	1.02E+03

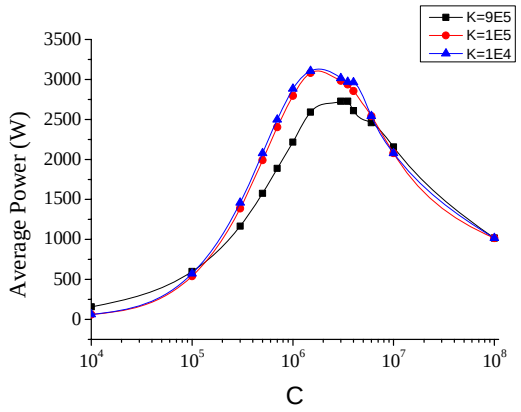

Fig. 13 Average power—Hinged damping

It can be predicted that the changes of average power are not obvious when K<9E5 by combining Fig. 9 with 10. And average power reaches maximum when C changes from 1.5E6 to 4E6. So magnitude of K is suggested to be less than or equal to 105. C is suggested to be 1.5E6~4E6.

In conclusion, the appropriate diameter can be achieved combined with cost control. If the section is ellipse, minor axes should be determined according to the requirement of equipment arrangement, and major axes can be achieved. The draft is 0.5D or 0.7D. It is suggested that hinged stiffness K<9E5, hinged damping is between 1.5E6 and 4E6.

V. COMPARING WITH EXPERIMENT RESULTS

To verify the accuracy of the power obtained in this paper, numerical simulation results are compared with 20th scale Glasgow University tests [14]. The 20th scale model is configured with 5 cylindrical units: 931mm (front); 3×846mm; 991m(rear), of 180mm diameter. A 250mm long drooped conical nose is attached to the front unit. The mooring system is the same with the system in this paper, lines are attached to the first and forth structure.

TABLE IX
COMPARISON BETWEEN THE NUMERICAL SIMULATION AND TEST RESULTS

TEST	T[s]	A[m]	λ [m]
H1	8.94	0.59	122
H2	8.94	1.22	122
H3	8.94	1.81	122
H4	8.94	2.36	122
M1	7.53	0.74	88
M2	7.53	1.54	88
M3	7.53	2.23	88
L1	6.5	0.82	66
L2	6.5	1.65	66
L3	6.5	2.43	66
L4	6.5	3.07	66
TEST	Exp.Power [KW]	Num.Power [KW]	Exp/num Power
H1	20.4	33.78	0.6
H2	84.6	115.17	0.73
H3	233.7	319.66	0.73
H4	443.3	629.61	0.7
M1	96.9	94.87	1.02
M2	426.1	528.32	0.81
M3	852.9	1015.05	0.84
L1	140.1	116.58	1.2
L2	503.2	528.37	0.95
L3	839.1	907.58	0.92
L4	1167.4	950.4	1.23

Table IX gives the experimental and numerical results for the total power absorbed. It can be seen that the ratio of power of tests and numerical simulation is 0.6~1.23. The feasibility and validity of this method is validated.

VI. CONCLUSIONS

Frequency domain analysis of the Pelamis WEC hydrodynamics has been developed and used to assess the power performance of the device in irregular incident waves. The optimum parameters of the device in Zhejiang Province have been obtained. In spite of somewhat simplifying assumptions, the obtained results are believed to be significant.

1) The heave and sway RAO, the key factors to the generated power, should be a serious consideration.
2) At some extent, the generated power increases with the increase of the diameter. The wave capture width and rotational inertia increase with diameter increasing. Then it will change the motion and power performance.
3) Keeping the cross-sectional area fixed, the larger axial ratio means the larger generated power. In reality, however, we should consider the limit of equipment arrangements.
4) Water plane stiffness decreases with draft increasing, so the relative motion is more severe. Considering the unsinkability and stability of device and little power increment of larger draft, it is suggested that the draft is 0.5D to 0.6D.
5) Considering the hinged stiffness and damping have a great effect on generated power, we should find the optimal values of K and C based on the actual structures and

operation state. For the benchmark device in the paper, it is suggested that hinged stiffness K<9E5, hinged damping is between 1.5E6 and 4E6.

ACKNOWLEDGMENT

This paper is funded by the International Exchange Program of Harbin Engineering University for Innovation-oriented Talents Cultivation.

REFERENCES

[1] A. Babarit, J. Hals, M.J. Muliawan(2012). Numerical benchmarking study of a selection of wave energy converters. Renewable Energy, 6(7), 131~142.
[2] Meyer NI, McDonalArnskov M, VadBennetzen CE, etc(2002). Bølgekraftprogram, Afslutningsrapport, Virum, Denmark RAMBØLL, Teknikerbyen 31, 2830.
[3] Previsic M, Bedard R, Hagerman G(2002). E2I EPRI assessment, offshore wave energy conversion devices. Electricity Innovation Institute;Technical report E2I EPRI WP - 004 - US - Rev 1.
[4] Manases(2010). Dynamics and hydrodynamics for floating wave energy converters. Ph.D. thesis, Lisboa University, Lisboa.52~59
[5] Nicolai F. HEILSKOV and Jacob V(2012). A non-linear numerical test bed for floating wave energy converters. Book of extended abstracts for the 2nd SDWED Symposium, Copenhagen 524-532.
[6] Newman J N(1994). Wave effects on deformable bodies .Applied Ocean Research, 16: 47~59.
[7] Gou Ying, TengBin(2004). Interaction effects between wave and two connected floating bodies. Engineering Science, 6(7), 75~80.
[8] L. Sun, R. Eatock Taylor and Y.S. Choo (2011). Responses of interconnected floating bodies. The IES Journal Part A: Civil & Structural Engineering, 4(3), 143–156
[9] Chuankun Wang, Wei Lu (2009) Analysis on ocean energy resources and storage, Ocean press, Beijing, China, 110-116
[10] Qin Ye, Zhongliang Yang, Weiyong Shi(2012), The preliminary research on the offshore wave energy resources in Zhejiang province, Journal of Marine Sciences, 30(4) 13-19
[11] J.N.Newman (1986). Marine Hydrodynamic. Massachusetts Institute of Technology Press, Massachusetts, America, 40-45
[12] Yishan Dai, WenyangDuan(2008). Potential Flow Theory of Ship Motions in Waves. National Defence Industry Press, Beijing, China,80-86
[13] Zhengban Sheng, YingzhongLiu(2003). Ship manoeuvring and seakeeping, Shanghai Jiao Tong University Press, Shanghai, China, 283-210.
[14] Pizer, D.J, Retzler, C.H.Yemm, R.W(2000). The OPD pelamis. Experimental and numerical results from the hydrodynamic work program. European wave energy conference, Aalborg (Denmark), 227-234.